Radiat Environ Biophys (2003) 42:49–53
DOI 10.1007/s00411-003-0185-8

ORIGINAL PAPER

D. Nikezic · K. N. Yu

Absorbed fraction of alpha-particles emitted in bifurcation regions of the human tracheo-bronchial tree

Received: 25 September 2002 / Accepted: 11 February 2003 / Published online: 8 April 2003

Abstract A model for bifurcation regions of the human tracheo-bronchial tree was developed. Equations for the surfaces are given to enable calculations of doses from alpha-particles emitted in these regions. It has been found that a bifurcation region is well approximated by a quasi-ellipsoid. The absorbed fractions of alpha-particles emitted in bifurcation regions were calculated by the Monte Carlo method. The average absorbed fraction under the bifurcation geometry is close to that found under the cylindrical geometry in the bronchial region. In the bronchiolar region, the absorbed fractions under the bifurcation geometry are up to 20% larger than those under the cylindrical geometry.

Introduction

The bifurcation geometry of airway tubes in the human tracheo-bronchial (T-B) tree has been considered for modeling aerosol deposition [1, 2], the latter mainly modeled by software developed using fluid dynamics [3, 4, 5]. There are theoretical findings [6] as well as experimental evidence of enhanced deposition in bifurcation regions. To calculate the absorbed dose in these regions due to radon progeny, one needs to know the absorbed fraction (AF) of alpha-particles in the bifurcation regions. The absorbed fraction is defined as the fraction of alpha-particle energy absorbed in the target. The AFs have been calculated for various target/source combinations and alpha energies and have been given in Annex H of ICRP publication 66 [7]. However, these data were obtained for the cylindrical geometry in which both the sources and targets were represented by long straight cylinders.

Although the bifurcation of a cylinder into two has previously been considered for deposition modeling, there is still no detailed analytical description of the bifurcation geometry. Computer simulations of the lung airways were performed by Spencer et al. [8], and a two-dimensional but pulsatile model of aortic bifurcation was employed by Chakravarty and Mandal [9]. In fact, it is not geometrically possible to split one cylinder into two without some distortion of the parent one in the bifurcation region. In the first part of this paper, we will present our model of a bifurcation. In the second part, the AFs of alpha-energy emitted in bifurcation regions will be given. These results can be used to calculate the absorbed dose when the activity of radon progeny in such a region is known.

Model of bifurcation geometry

The model of a symmetrical bifurcation is presented in Fig. 1. The nomenclature is as follows: U upper cylinder that bifurcates and r_u its radius, L lower left branch of the bifurcation, and r_L its radius, α the angle of bifurcation, (x, y, z) the coordinate system with the origin O on the axis of cylinder U in the plane where bifurcation occurs, in which the z-axis is along the axis of U and the y-axis chosen in such a way that the axes of U and L are in the y-z plane. In other words, the bifurcation occurs in the y-z plane, while the x-axis is normal to the plane of the paper. Both U and L are intersected by the plane π which is parallel to the x-axis and which subtends an angle β to the z-axis (the cross-section between the cylinder and the plane is an ellipse). The angle β is chosen to fulfil the condition $a_L = a_U/2$, where a_L is the major-axis of the ellipse formed by the intersection of L and π, and a_U is the corresponding value of the ellipse formed by the intersection of U and π (not shown in Fig. 1).

When a cylinder intersects the plane at an angle β, we have:

K. N. Yu (✉)
Department of Physics and Materials Science,
City University of Hong Kong,
Tat Chee Avenue, Kowloon Tong, Kowloon, Hong Kong
e-mail: peter.yu@cityu.edu.hk

D. Nikezic
Faculty of Science, University of Kragujevac,
34000 Kragujevac, Yugoslavia

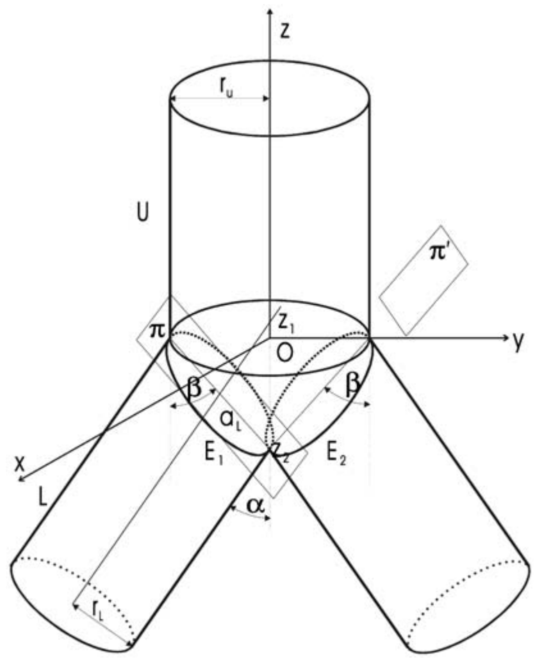

Fig. 1 Model of symmetrical branching of one cylinder into two

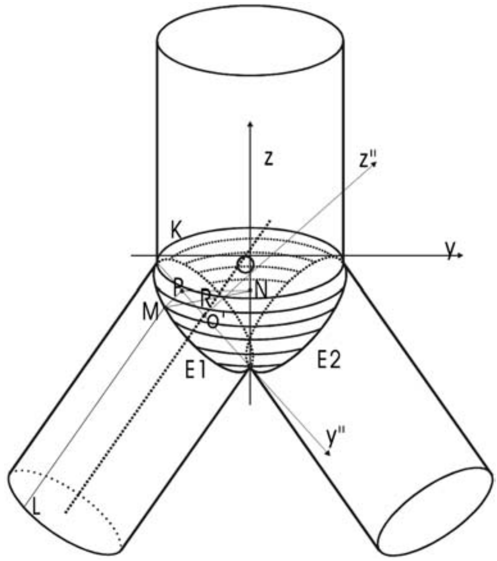

Fig. 2 Construction of a bifurcation region (marked with parallel horizontal lines). Point M is on the ellipse E_1 (with O' as the center); it rotates around the z-axis to form a circle with radius R centered at point N

$$a_U = \frac{r_U}{\sin\beta} \tag{1}$$

Since π does not intersect the axis of L at a right angle, $a_L \neq r_L$. Under geometrical conditions one can obtain:

$$a_L = \frac{r_L}{\sin(\alpha+\beta)} \tag{2}$$

On combining Eqs. 1 and 2, and using $a_L = a_U/2$, we have:

$$ctg\beta = \frac{2\frac{r_L}{r_U} - \cos\alpha}{\sin a} \tag{3}$$

In this way, the angle β is determined by the radii r_L and r_U, and the bifurcation angle α. The following explains some more notations in Fig. 1: the axis of L intersects the z-axis at z_1, at the same point the axis of the lower right cylinder intersects the z-axis. The plane π intersects the z-axis at z_2. The two coordinates can be found from:

$$z_1 = \frac{r_U\cos\alpha - r_L}{\sin\alpha}; z_2 = \frac{r_U}{\tan\beta} \tag{4}$$

The equations for the lower cylinders are:

$$x^2 + [\pm y\cos\alpha + (z - z_1)\sin\alpha]^2 = r_L^2 \tag{5}$$

where the "+" and "–" signs are for the right and left cylinders, respectively. The intersection between the plane π and L is the ellipse E_1. The plane π', which is symmetrical to π with respect to the z-axis, intersects the lower right cylinder to form the ellipse E_2.

The "bifurcation region" is depicted by the surface with parallel horizontal circular lines in Fig. 2. This surface is constructed by rotating the edge of ellipse E_1 around the z-axis. The surface thus depicted defines the bifurcation region. Consider the line LM which is on the surface of the lower left tube (the axis of that tube is also shown in Fig. 2 with a dashed line). The intersection between LM and E_1 is the point M. The point N on the z-axis is the horizontal projection of M onto the z-axis. When the point M is rotated around the z-axis, a circle is drawn with the distance NM as the radius. When all points on E_1 are considered, all the circles formed will define the bifurcation region. The generated surface of the bifurcation region is not a "standard ellipsoid" because the latter is formed when an ellipse revolves around one of its axes. In our case, the ellipse is revolved around the z-axis which does not coincide with an axis of the ellipse.

The task to be solved is to find the equation of the surface of this bifurcation region. It is necessary to make a two-step transformation of the coordinate system. The first step translates the origin from O to O' while the second rotates the system around the x-axis for an angle $-(\pi/2-\beta)$; with the "–" sign outside the bracket meaning a clockwise rotation, while a "+"sign will mean an anticlockwise rotation. The final coordinate system (x'', y'', z'') has a z''-axis normal to the plane of ellipse E_1, which is not the axis of the cylinder. The y''-axis is along the major axis and the x''-axis is along the minor axis of E_1. The relationship among the coordinates in the (x, y, z) and (x'', y'', z'') systems are obtained in the following:

The equation of the plane π in the (x, y, z) system is:

$$(y + r_U)\cos\beta + z\sin\beta = 0 \tag{6}$$

The axis of the lower left cylinder is:

$$z = y\cot\alpha + z_1 \tag{7}$$

The intersection between this line and the plane π can be found by combining Eqs. 6 and 7, which gives the coordinates (0, y_{int}, z_{int}) of the point *O'* in the (x, y, z) system:

$$y_{\mathrm{int}} = \frac{-z_1 \sin\beta - r_U \cos\beta}{\sin\beta \cot\alpha + \cos\beta} \tag{8}$$

$$z_{\mathrm{int}} = \cot\alpha \cdot y_{\mathrm{int}} + z_1 \tag{9}$$

The first step is the translation of the origin from O to O'. The new axes become:

$$y' = y - y_{\mathrm{int}} \text{ and } z' = z - z_{\mathrm{int}} \tag{10}$$

The plane π in the translated system is:

$$(y' + y_{\mathrm{int}} + r_U)\cos\beta + (z' + z_{\mathrm{int}})\sin\beta = 0 \tag{11}$$

The second transformation is a rotation around the x-axis for an angle of $-(\pi/2-\beta)$.

The transformations from the (x, y, z) system to the "translated + rotated system" are expressed as:

$$\begin{aligned} y &= y''\sin\beta + z''\cos\beta + y_{\mathrm{int}} \\ z &= -y''\cos\beta + z''\sin\beta + z_{\mathrm{int}} \end{aligned} \tag{12}$$

and vice versa as:

$$\begin{aligned} y'' &= (y - y_{\mathrm{int}})\sin\beta - (z - z_{\mathrm{int}})\cos\beta \\ z'' &= (y - y_{\mathrm{int}})\cos\beta + (z - z_{\mathrm{int}})\sin\beta \end{aligned} \tag{13}$$

The equation of the plane π in the (x'', y'',z'') system is z''=0. The equations of the cylinders have to be transformed in the (x'', y'',z'') system to find the intersection between cylinders and the plane. The intersection is an ellipse E_1 with the equation:

$$\frac{x^2}{r_L^2} + \frac{y''^2}{(r_L/\sin(\alpha+\beta))^2} = 1 \tag{14}$$

in the (x'', y'',z'') system.

The equation of the ellipse E_1 in the (x, y, z) system is now:

$$\frac{x^2}{r_L^2} + \frac{[(y - y_{cross})\sin\beta - (z - z_{cross})\cos\beta]^2}{(r_L/\sin(\alpha+\beta))^2} = 1 \tag{15}$$

The details of the rotation of the ellipse E_1 around the z-axis are presented in Fig. 3.

For a point N on the z-axis with a given z value, we can calculate the distance to the point M on the ellipse (points M and N are on the same horizontal plane defined by z; see Fig. 2). The distance MN is the radius R of a circle when the ellipse is rotated around the z-axis.

The y coordinate of point M is the same as that of point P in Fig. 2, which can be found from Eq. 6 as:

$$y_M = -r_U - z\tan\beta \tag{16}$$

Then the x coordinate of point M (from the equation for E_1) is:

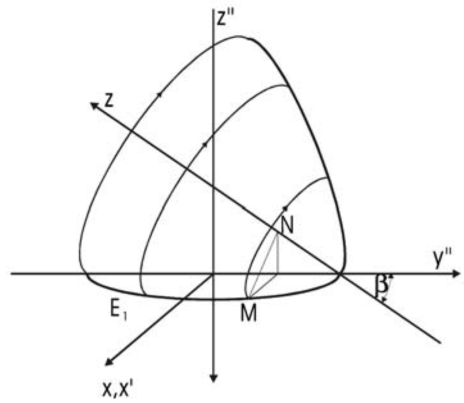

Fig. 3 Rotation of the ellipse E_1 around the z-axis

$$x_M = r_L\sqrt{1 - \frac{[(-r_U - z\tan\beta - y_{cross})\sin\beta}{[r_L/\sin(\alpha+\beta)]^2} \cdot \frac{-(z - z_{cross})\cos\beta]^2}{[r_L/\sin(\alpha+\beta)]^2}} \tag{17}$$

The radius R of the circle is:

$$R^2 = x_M^2 + y_M^2 \tag{18}$$

Since $y_M = -r_U - z\tan\beta$, one can find:

$$R = \sqrt{r_L^2\left(1 - \frac{[(-r_U - z\tan\beta - y_{cross})\sin\beta}{[r_L/\sin(\alpha+\beta)]^2} \cdot \frac{-(z - z_{cross})\cos\beta]^2}{[r_L/\sin(\alpha+\beta)]^2}\right) + (-r_U - z\tan\beta)^2} \tag{19}$$

The function $R=R(z)$ is obtained in this way. Finally, the equation of the surface obtained is:

$$x^2 + y^2 = R^2(z) \tag{20}$$

where $R(z)$ is given above in Eq. 19.

Equation 19 was programmed and the results calculated for the first 8 generations of the human T-B tree (see Fig. 4). The bifurcation regions can be obtained by rotating the curves in Fig. 4 around the z-axis.

Absorbed fraction of alpha-energy emitted in bifurcation regions

The geometry of a bifurcation region is significantly different from the cylindrical geometry that was previously assumed in AF calculations in the ICRP66 report. The geometry described by Eq. 19 resembles an ellipsoid and we refer to it as a "quasi-ellipsoid". In addition to the significant difference in the geometries, alpha-particles travelling through the air can now enter one of the three cylinders (upper, lower left or lower right) surrounding the considered region. All these cases are carefully considered in the computer programs.

Table 1 Absorbed fraction from alpha-particles emitted in bifurcation regions

Source	Method and generation of T-B tree		Bronchial region (BB)			
			Secretory cells		Basal cells	
			6 MeV	7.69 MeV	6 MeV	7.69 MeV
Fast mucus	ICRP66	→	0.249	0.353	5×10^{-3}	0.0893
		Gen ↓				
	This work	1	0.209	0.342	3.2×10^{-3}	0.069
		2	0.223	0.352	4.1×10^{-3}	0.073
		3	0.229	0.358	2.8×10^{-3}	0.074
		4	0.248	0.355	3.8×10^{-3}	0.088
		5	0.260	0.364	3.8×10^{-3}	0.093
		6	0.255	0.377	3.0×10^{-3}	0.089
		7	0.262	0.382	3.8×10^{-3}	0.093
		8	0.270	0.386	3.2×10^{-3}	0.0922
		Mean	0.244	0.364	3.5×10^{-3}	0.0839
Slow mucus	ICRP66	→	0.272	0.355	0.021	0.0857
		Gen ↓				
	This work	1	0.258	0.332	0.0215	0.0760
		2	0.255	0.345	0.0202	0.0703
		3	0.250	0.347	0.0179	0.0726
		4	0.291	0.363	0.0234	0.0895
		5	0.278	0.350	0.0245	0.0855
		6	0.288	0.378	0.0208	0.0880
		7	0.290	0.381	0.0214	0.0888
		8	0.278	0.370	0.0183	0.0858
		Mean	0.273	0.358	0.021	0.0821

Source	Method and generation of T-B tree		Bronchiolar region (bb) (secretory cells only)	
			Secretory cells	
			6 MeV	7.69 MeV
			0.217	0.173
Fast mucus	ICRP66	→	0.214	0.172
		Gen ↓		
	This work	9	0.232	0.179
		10	0.233	0.183
		11	0.244	0.177
		12	0.299	0.178
		13	0.299	0.177
		14	0.224	0.170
		15	0.219	0.180
		Mean	0.250	0.178
Slow mucus	ICRP66	→	0.217	0.173
		Gen ↓		
	This work	9	0.231	0.196
		10	0.228	0.199
		11	0.228	0.199
		12	0.227	0.202
		13	0.240	0.205
		14	0.236	0.204
		15	0.245	0.201
		Mean	0.234	0.201

To calculate AFs, we only consider alpha-particles emitted in bifurcation regions. Therefore, the results given below are only related to the bifurcation regions, and not to the entire T-B tree. For the present study, a uniform distribution of alpha contamination in the mucus was employed. Previously developed programs for the cylindrical geometry based on Monte Carlo methods [10] were modified for the considered quasi-ellipsoid. A detailed description of the program is not repeated here.

The ICRP66 model of the T-B tree was partially adopted: the wall of the airway tube was the same as that described by ICRP66. Two sources (fast and slow clearing mucus) and two targets (secretory and basal cells) and two relevant alpha energies in the ^{222}Rn chain (6 and 7.69 MeV) were considered. However, the calculations were performed for each particular generation. The diameters and lengths of tubes, as well as branching angles given in ICRP66 for the purpose of

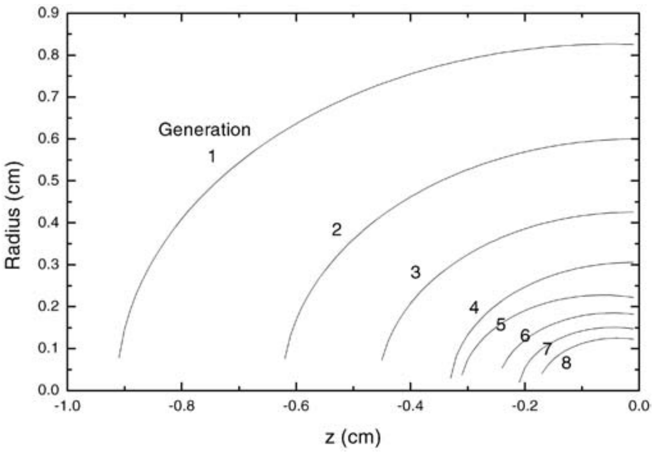

Fig. 4 Radius vs. depth from the plane where branching started for the first 6 generations of the human respiratory tract. The radii for z=0 are those of the tubes for the corresponding generations. The points where the curves drop to zero (e.g., z=–0.93 for generation 1) is the depth z_2 of the bifurcation region

deposition calculations, were adopted here for AF calculations.

The results for AF are given in Table 1. For easier comparison, the ICRP66 values are italicized. Inspection of these results reveal that in most cases, AFs from alpha-particles emitted in bifurcation regions are larger than ICRP66 values. The differences are particularly pronounced for larger generation numbers. The only exception is the dose in basal cells from 6 MeV alpha-particles emitted in fast mucus. This exception is not important because that value of AF is two orders of magnitude smaller than the others. Previously, the bifurcation regions were considered as "hot spots" for particle deposition. Calculations performed here indicate that the doses around bifurcation regions could be even larger because the AFs are larger in the quasi-ellipsoidal geometry than those in cylindrical geometry.

Conclusions

Absorbed fractions of alpha-particles emitted in bifurcation regions are given in Table 1 for different generation numbers in the human tracheo-bronchial tree. The average values of AFs are also given in Table 1. In the bronchial region, the AFs under the bifurcation geometry are close to those recommended by ICRP66 for infinitely long cylindrical tubes. On the other hand, the AFs in the bronchiolar region under the bifurcation geometry are up to 20% larger than those under the cylindrical geometry. The effect of particles emitted in the bifurcation regions on the total dose depends on the number of alpha decays in these regions (which might not be equal to the number of deposited atoms because of the clearance and translocations of deposited materials).

Acknowledgment This work is supported by the CERG grant CityU1004/99P from the Research Grant Council of Hong Kong.

References

1. Hofmann W, Balashazy I, Koblinger L (1995) The effect of gravity on particle deposition patterns in bronchial airway bifurcations. J Aerosol Sci 26:1161–1168
2. Hofmann W, Balashazy I, Heistracher T (2001) The relationship between secondary flows and particle deposition patterns in airway bifurcations. Aerosol Sci Technol 35:958–968
3. Martonen TB, Guan X, Schreck RM (2001) Fluid dynamics in airway bifurcations. I. Primary flows. Inhal Toxicol 13:261–279
4. Martonen TB, Guan X, Schreck RM (2001) Fluid dynamics in airway bifurcations. II. Secondary currents. Inhal Toxicol 13:281–289
5. Martonen TB, Guan X, Schreck RM (2001) Fluid dynamics in airway bifurcations. III. Localized flow conditions. Inhal Toxicol 13:291–305
6. Balashazy I, Hofmann W (2000) Quantification of local deposition patterns of inhaled radon decay products in human bronchial airway bifurcations. Health Phys 78:147–158
7. ICRP (1994) ICRP Publication 66. Human respiratory tract model for radiological protection. A report of a Task Group of the International Commission on Radiological Protection. Pergamon Press, New York
8. Spencer RM, Schroeter JD, Martonen TB (2001) Computer simulations of lung airway structures using data-driven surface modeling techniques. Comput Biol Med 31:499–511
9. Chakravarty S, Mandal PK (1997) An analysis of pulsatile flow in a model aortic bifurcation. Int J Eng Sci 35:409–422
10. Nikezic D, Yu KN (2002) Distributions of specific energy in sensitive layers of the human respiratory tract. Radiat Res 157:92–98